Sensory and Motor Systems

Taste-Odor Association Learning Alters the Dynamics of Intraoral Odor Responses in the Posterior Piriform Cortex of Awake Rats

Joost X. Maier, Ammar Idris, and Brooke A. Christensen

Department of Neurobiology and Anatomy, Wake Forest Atrium Baptist Medical Center, Winston-Salem, NC 27157

Abstract

How an odor is perceived is to a large extent dependent on the context in which that odor is (or has been) experienced. For example, experiencing an odor in mixture with taste during consumption can instill taste qualities in the percept of that odor (e.g., vanilla, an odor, has a gustatory quality: sweet). How associative features of odors are encoded in the brain remains unknown, but previous work suggests an important role for ongoing interactions between piriform cortex and extraolfactory systems. Here, we tested the hypothesis that piriform cortex dynamically encodes taste associations of odors. Rats were trained to associate one of two odors with saccharin; the other odor remained neutral. Before and after training, we tested preferences for the saccharin-associated odor versus the neutral odor, and recorded spiking responses from ensembles of neurons in posterior piriform cortex (pPC) to intraoral delivery of small drops of the same odor solutions. The results show that animals successfully learned taste-odor associations. At the neural level, single pPC neuron responses to the saccharin-paired odor were selectively altered following conditioning. Altered response patterns appeared after 1 s following stimulus delivery, and successfully discriminated between the two odors. However, firing rate patterns in the late epoch appeared different from firing rates early in the early epoch ($<$1 s following stimulus delivery). That is, in different response epoch, neurons used different codes to represent the difference between the two odors. The same dynamic coding scheme was observed at the ensemble level.

Key words: olfactory cortex; taste; smell; flavor; retronasal; decoding

---

Significance Statement

Odors carry important meaning beyond their chemical identity. One particularly salient example of this are food odors, which play an important role in determining flavor preferences and food choice behavior. How these extra-olfactory aspects of odor are represented is unknown. Using extracellular recordings in awake rats in the context of a flavor preference learning task, we show that learned taste associations of odor stimuli are represented in the dynamic firing patterns of posterior piriform cortex (pPC) neurons. The results suggest that associative odor coding results from ongoing interactions between olfactory and extraolfactory systems.

Introduction

Smell is unique among the senses in that it faces an extraordinary large number of potential sensory qualities (Bushdid et al., 2014). To meet this challenge, olfactory space is not represented in fixed, topographically organized maps as in other sensory systems (Rennaker et al., 2007; Stettler and Axel, 2009). Instead, cortical odor coding is highly plastic and depends to a large extent on the context in which an individual experiences an odor (Wilson and Stevenson, 2003; Wilson et al., 2004).

One particularly salient context in which olfaction plays a major role is consumption. During consumption, odor stimuli are typically experienced in mixture with taste.

Behavioral work has shown that interactions between taste and odor components of flavor are highly adaptive in informing consumption decisions (Holman, 1975; Sclafani and Ackroff, 1994; Slotnick et al., 1997; Blankenship et al., 2019; Elliott and Maier, 2020; Maier and Elliott, 2020). One example of taste-odor interactions during consumption is the formation of taste-odor associations. Odors experienced in mixture with taste acquire qualities associated with that taste (Stevenson et al., 1995, 1998, 2000a, b; Stevenson and Boakes, 2004; Yeomans et al., 2006; McQueen et al., 2020). Taste-odor association learning is robust, rapid, and affects subsequent consumption behavior: odors that have been experienced in mixture with palatable tastes become attractive.

Recent work aimed at elucidating how taste-odor associations are represented in the brain has indicated a role for the insular gustatory cortex (GC). Optogenetic inhibition of GC after rats learned to associate an odor with saccharin (a sweet taste) impaired their ability to express a preference for that odor (Maier et al., 2015; Blankenship et al., 2019). However, how GC exerts its effect on neural coding of taste-odor associations is unknown. Taste-odor associations may reside locally in GC. Alternatively, GC may support taste-odor associations by modulating sensory processing in olfactory areas. One potential area through which GC may affect olfactory processing is the piriform (olfactory) cortex, a large cortical surface that receives bottom-up input from the olfactory bulb representing a vast space of odorant molecules (Scott et al., 1980; Schwob and Price, 1984; Rennaker et al., 2007; Stettler and Axel, 2009; Miyamichi et al., 2011; Sosulski et al., 2011). Moreover, the piriform cortex is ideally situated to interact with extraolfactory systems (Luskin and Price, 1983; Johnson et al., 2000; Haberly, 2001; Majak et al., 2004; Sadrian and Wilson, 2015), sculpting odor representations based on the context an odor is encountered in (Kadohisa and Wilson, 2006; W. Li et al., 2006, 2008; Calu et al., 2007; Roesch et al., 2007; Barnes et al., 2011; Chen et al., 2011; Chapuis and Wilson, 2012; Gire et al., 2013; Meissner-Bernard et al., 2019; D. Wang et al., 2019). Interactions with extraolfactory systems are particularly pronounced in the posterior piriform cortex (pPC; Johnson et al., 2000; Majak et al., 2004; Zelano et al., 2005; W. Li et al., 2006; Calu et al., 2007). Indeed, pPC odor representations have been shown to be affected by experience and multisensory context (Karunanayaka et al., 2015; Avery et al., 2020). Previous work from our lab identified GC as a source of extraolfactory input to pPC, as inactivation of GC affects pPC responses to taste stimuli, as well as odor stimuli even in the absence of concurrent taste input (Maier et al., 2015). Together, these findings suggest that encoding of taste-odor associations may be supported by ongoing interactions between GC and pPC.

Here, we test the hypothesis that taste associations of odor stimuli are represented in pPC. Specifically, we predict that experience with taste-smell mixtures affects responses of pPC neurons to intraoral delivery of odor solutions. We further predict that the effect of experience is reflected in changes in response dynamics, consistent with the idea that odor coding in the context of consumption depends on ongoing interactions with the taste system. Alternatively, if taste associations are represented locally in GC, we do not predict any experience-dependent changes in responsiveness at the level of pPC. Associations may also be represented locally in pPC, independently of GC. In this case, we expect experience to be reflected in static pPC response patterns. To test our predictions regarding neural coding of taste-odor associations, we used extracellular electrophysiology to record spiking activity from ensembles of single pPC neurons of awake rats while they consumed odor solutions, before and after taste-odor association learning. We show that taste-odor association learning changes the temporal dynamics of odor responses, such that initial odor-selective response patterns are transformed over the course of seconds into a novel representation that distinguishes taste-associated from taste-naive odors. These results suggest that pPC dynamically encodes both odor identity and taste association.

Materials and Methods

Subjects

A total of 30 adult female Long–Evans rats (Charles River), weighing between 250 and 300 g at the time of surgery served as subjects. All rats were individually housed and kept on a 12/12 h light/dark cycle [zeitgeber time 0 = 6 A.M.]. Experiments were conducted during the light cycle. All animal procedures were performed in accordance with the Wake Forest Atrium Baptist Medical Center animal care committee's regulations.

Surgery

Animals were injected intraperitoneally with the analgesic meloxicam (10 mg/kg) before surgery. Stereotaxic surgery was performed under intranasally administered isoflurane anesthesia (2–5%). First, the scalp was treated with lidocaine ointment, an incision was made, and the skin retracted from the skull. Using a dental drill, a craniotomy was made overlying the posterior piriform olfactory cortex (unilateral or bilateral): 1.4 mm posterior to bregma, 5.2–5.6 mm lateral to the midline, 6.4–7.4 mm ventral from the surface of the brain (Paxinos and Watson, 1986). Five additional burr holes were made, evenly spread across the skull, for the insertion of skull screws that provide stability to the implant. Electrodes were then lowered to the piriform cortex over the course of 30 min using a manually-driven stereotaxic arm. Once in place, the craniotomy was

filled with Kwik-Cast (World Precision Instruments), and the electrode connector and skull screws were covered in dental acrylic, fixing the electrodes in place. Electrode assemblies consisted of micro-wire arrays with 6 or 8 electrodes in circular arrangement, or 16 electrodes in square arrangement. Electrodes were 25-µm diameter stainless steel wires, spaced 100–200 µm apart (MicroProbes), or multielectrode silicon probes (two shanks of 16 electrode contacts each, shanks spaced 500 µm apart; electrode contacts spaced 50 µm apart, NeuroNexus model A2x16-10 mm-50-500-177-CM32). Intraoral cannulae (IOC) were implanted to provide access to the oral cavity (Phillips and Norgren, 1970): flanged microbore PE tubing (1.143 mm ID, 1.574 mm OD) was inserted behind the second molar using a 20-G needle, and guided under the skin overlying the zygomatic arch to exit at the edge of the cranial implant. Tubing was then attached to a coupler body (CPC, #SMF01) that could interface with a counterpart holding a manifold of fluid delivery tubes. Once in place, the coupler was secured to the rest of the implant with dental acrylic. Animals recovered in their home cage with *ad libitum* access to water and mashed rat chow for 4–5 d after surgery before the start of the experiment.

Stimuli

Unisensory odor stimuli were exemplars of monomolecular odorants (obtained from Sigma-Aldrich; >98% purity) that have been used in similar behavioral (Blankenship et al., 2019) and neural recording (Maier, 2017) paradigms in previous studies: methyl valerate and 2-hexanone in aqueous solution (0.025% volume/volume in distilled water). Saccharin (0.2%; Fisher Scientific) was used as an unconditioned stimulus during conditioning sessions. All stimuli were presented intraorally to allow, as much as possible, natural sensory stimulation dynamics associated with intraoral evaluation of flavor. There is no empirical evidence that the odorants used here completely lack gustatory and/or trigeminal qualities. However, similar concentrations of odor solutions have been shown to be below nonolfactory behavioral detection thresholds (Slotnick et al., 1997; Gautam and Verhagen, 2012) and are therefore unlikely to have contributed to the observed responses.

Behavioral procedures

Preference testing

Two-bottle tests were used to assess odor preferences before and after conditioning. During each preference testing session, animals were given free access to two odor solutions overnight (6 P.M. to 8 A.M.). Animals received *ad libitum* access to water in between two-bottle tests, ensuring that they were never deprived of fluid during preference testing sessions. Relative position of the odor bottles in the cage was alternated between sessions and counterbalanced across rats. In one preference test, consumption from one bottle could not be determined because of spillage (0.8% of all bottles); data from this animal were excluded from contributing to the behavioral dataset.

Conditioning

One-bottle access was used for conditioning, performed over four consecutive days. Each morning (10 A.M.), animals had access to 10 ml of one of the odors (odor A) in plain water, or the other odor (odor B) in saccharin solution for 30 min. Bottles alternated on an A-B-A-B schedule, and the identity of odors A and B (methyl valerate or 2-hexanone) was counterbalanced across rats.

Stimulus presentation and recording procedures

The recording arena consisted of a $29 \times 23 \times 33$ cm Plexiglas chamber encased in metal that served as a Faraday cage. Stimuli were delivered via syringe pumps directly onto the dorsal surface of the tongue while animals were moving freely around the arena. Syringes containing stimulus solution were connected to blunted needles fitted with strands of PE tubing (1.143 mm ID, 1.574 mm OD) that fed into the recording arena via an opening in the roof. At the distal end of each strand of PE tubing, a 5 cm strand of PI microbore tubing (0.0254 mm ID, 0.0270 mm OD) was glued, and all tubes were inserted into the through hole of a coupler body (CPC, #SMF02) and held together with glue. Before experimental sessions, the collection of PI tubes was fed into the IOC and secured in place by mating the coupler bodies on the tube manifold and IOC. Once connected, the tips of the PI tubes extended 0.5 mm below the tip of the IOC into the oral cavity. Animals were habituated to the recording setup and stimulus delivery apparatus before recording by presenting drops of water through IOC in the recording arena. During recording sessions, airborne odorants were cleared by a continuously running fan mounted in the ceiling of the recording arena. To encourage consumption of stimuli, animals were deprived of water for 6 h before recording sessions. During each recording session, odors A and B, as well as plain water were presented in random order (10 repetitions of each stimulus). Stimuli were always presented in random order. Intraoral stimuli were delivered in 30- to 50-µl aliquots (total duration of delivery <100 ms), with a random intertrial interval ranging from 30–45 s, allowing sufficient time for animals to swallow the fluid and clear their mouth. Each session yielded between 1 and 16 (mean = 5.0) single neurons (0.3 neurons/electrode on average). In a subset of animals, multisensory mixtures of odors A/B and taste compounds (saccharin and/or sodium chloride), as well as unisensory taste compounds in isolation, were presented in addition to the stimuli listed above (data not included in the present paper). During these sessions, both odorants were paired with the same tastant(s) for 10 trials per mixture. Recording and preference testing sessions were always performed according to the same schedule. Given the limited and balanced nature of mixture exposure during recording sessions, it is unlikely to have impacted the results reported in the present study. Results from a subset of recordings in response to mixtures have been reported previously (Idris et al., 2023).

Electrophysiological recording and data processing

The continuous extracellular signal recorded from each electrode was amplified, digitized and stored for offline analysis at a sampling rate of 25 kHz using INTAN RHD2000
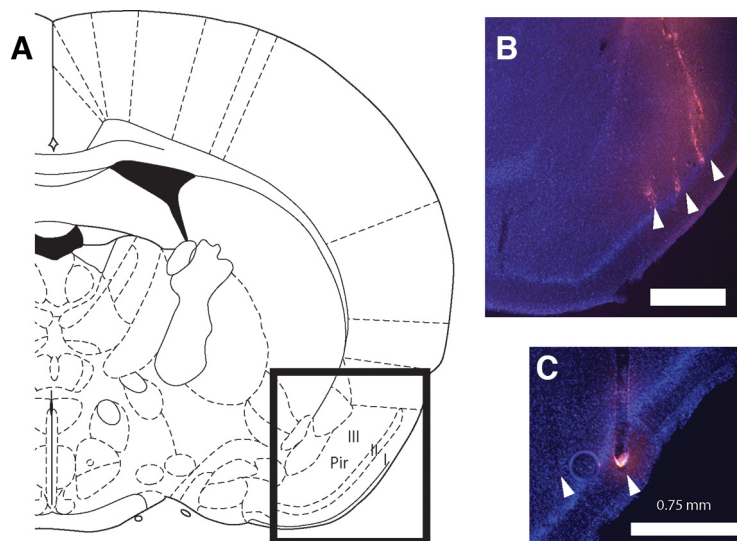
Figure 1. Histologic reconstruction of recording sites. ***A***, Schematic from a rat brain atlas (Paxinos and Watson, 1986) indicating the general region of the posterior piriform cortex Layers I, II, and III in a coronal view (1.4 mm posterior to bregma). ***B***, ***C***, Coronal sections taken from two rat brains showing DAPI (blue) and DiI (pink) staining of nuclei and electrode tracts, respectively. Scale bar indicates 0.75 mm. Electrode tips are indicated by arrowheads. Animal in ***B*** was implanted with a microwire array; animal in ***C*** with a silicon probe.

hardware and acquisition software (Intan Technologies). Action potentials were extracted, clustered and sorted using the klusta/phy toolbox to obtain single neuron spike time stamps (Rossant et al., 2016). For silicon probe recordings, spikes were clustered taking into account the possibility that the same action potentials could be recorded by up to three neighboring channels. Spike time stamps were then binned at 1-ms resolution and aligned to stimulus delivery before further analysis. Only action potentials that exceeded 3.5 SD units of the high-pass filtered (400 Hz) voltage signal were included in the clustering analysis, and only clusters that contained <2% of action potentials occurring at an interspike interval of 2 ms or less were included in the dataset (Gadziola et al., 2015).

Data analysis

Offline analyses were performed using MATLAB (MathWorks). For time-averaged analysis, responses were averaged over the following time windows relative to stimulus delivery: −2000–0 ms (baseline period), 0–2500 ms (total stimulus period), 0–1250 ms (early stimulus period), 1250–2500 ms (late stimulus period). For time-resolved analysis, responses were averaged in a sliding window over time (window size: 500 ms; step size: 50 ms). Cohen's d was calculated to provide a continuous measure of effect size (discriminability) for each neuron: Cohen's $d = (\text{mean}_A - \text{mean}_B)/\text{std}_{pooled}$, where $\text{std}_{pooled} = ([\text{std}_A{}^2 + \text{std}_B{}^2])/2$.

To make the connection between firing rates of individual neurons and the amount of information present in the collective responses of ensembles of neurons, we performed single-trial ensemble decoding analysis (Quiroga et al., 2007; Bolding and Franks, 2017). Specifically, we asked how well odors A and B could be discriminated based on the firing rates of all simultaneously-recorded single neurons during a given session. For each temporal

analysis window (i.e., baseline, stimulus, sliding window over time), we first computed single-trial ensemble response vectors, consisting of the time-averaged response in that window for each simultaneously-recorded neuron. Each single-trial ensemble response vector was then compared with two templates (A and B), consisting of the ensemble response vectors averaged across all odor A and odor B trials (excluding the trial to be decoded). Similarity of each trial to both templates was then quantified by calculating the Euclidean distance. Decoding accuracy was defined as the percentage of trials that showed greater similarity with the correct template (i.e., an ensemble response on an odor A trial showing higher similarity with the odor A template than with the odor B template, and vice versa).

Histology

Electrodes were labeled with a drop of Vybrant DiI cell-labeling solution (Thermo Fisher Scientific), applied with a needle tip before implantation, allowing postmortem reconstruction of the implant location. In order to do so, rats were perfused transcardially with saline and 10% formalin, their brains extracted and placed in 30% sucrose for 3–5 d. Brains were then frozen; coronal sections were cut around the implant location using a sliding microtome, mounted on glass slides in DAPI Fluoromount-G medium (Southern Biotech) and a coverslip was applied. Epifluorescence microscopy was used to visualize DiI and DAPI. Figure 1 shows histologic reconstruction of electrode placement in pPC for two representative animals.

Statistics

Statistical tests involved comparing distributions of quantities (preference, firing rate, effect size, decoding
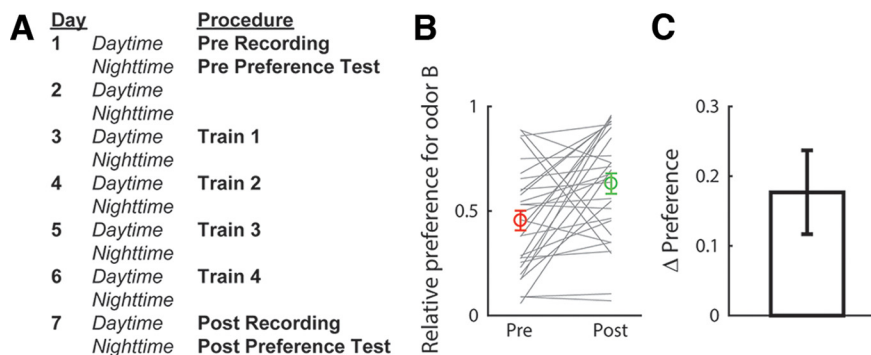
Figure 2. Odor-taste association paradigm. **A**, Sequence of procedures in the experimental paradigm. **B**, Preferences for the saccharin-paired odor (odor B) obtained before and after conditioning for each animal (gray lines). Averages ($\pm$SEM) over animals ($n = 29$) are shown in color. **C**, Change in preference (post–pre conditioning), averaged ($\pm$SEM) over animals.

accuracy) over animals, trials, neurons, or sessions These distributions followed approximately normal distributions. Repeated measures (i.e., preference pre and post conditioning, activity during stimulus and baseline periods) were compared using a paired samples t test. Other comparisons were performed using an independent samples t test. Similarly, factors in ANOVA were treated as within-subjects or between-subjects as applicable. Frequency of occurrence was compared between conditions using nonparametric sign-test or χ^2 test. All tests were two-tailed with $\alpha = 0.05$.

Results

Behavioral assessment of taste-odor association learning

The present study aimed to elucidate the neural representation of taste-odor associations. In particular, we tested the hypothesis that taste associations of odors are encoded in the activity of pPC neurons via ongoing top-down modulations. Odor-taste association learning was established and assessed using a two-bottle consumption task in which we measured relative preference for a test odor B versus a control odor A, before and after animals learned to associate odor B with 0.2% saccharin (a palatable sweet taste). An outline of the experimental protocol is shown in Figure 2A. Figure 2B shows preferences for odor B (relative to odor A) before and after conditioning. After conditioning, a significant majority of animals (23 out of 29, 79%, sign test: $p < 0.01$) increased their preference for the saccharin-paired odor (t test comparing preferences before and after conditioning: $t_{(28)} = 2.94$, $p < 0.01$; Fig. 2C). Thus, our training procedure was effective in conditioning a preference for the saccharin-paired odor relative to the control odor, consistent with previous work (Holman, 1975; Maier et al., 2015; Blankenship et al., 2019; Christensen et al., 2022).

Responsiveness of single pPC neurons to odor solutions

To investigate how neurons in pPC may encode taste-odor associations, we recorded responses from small ensembles of single pPC neurons to intraoral delivery of odor A and B solutions before and after preference learning. Stimuli were presented intraorally to allow, as much as possible, the natural dynamics of sensory stimulation that occurs during oral evaluation of flavor, including retronasal odorant delivery, concurrent somatosensory stimulation and orofacial behaviors associated with consumption. A total of 299 single neurons were isolated across the two recording sessions per animal ($n = 152$ and 147 neurons before and after conditioning, respectively). Figure 3 shows examples of single pPC neuron responses, highlighting the main patterns observed across the population. The neurons in Figure 3A,B were recorded before conditioning; the neurons in Figure 3C,D were recorded after conditioning. Responses were often odor selective [Fig. 3A,C,D, where responses differed between odors A and B as determined by independent samples t test comparing average responses in stimulus period (2.5-s window immediately following stimulus onset)]; responses typically exhibited sustained responses across the stimulus period; and could be excited (Fig. 3A,C) or inhibited (Fig. 3B) relative to baseline [as determined by paired samples t test comparing average responses in the stimulus period versus baseline (2.5 s immediately preceding stimulus onset)]. Some responses appeared to exhibit complex dynamics. For example, the response to odor B for the neuron shown in Figure 3D switched from being inhibited early in the response to being excited later in the response. In order to determine how pPC neurons may represent information about the odor stimuli, we first quantified the number of neurons that respond to each odor. Given the variable and protracted response dynamics observed in individual neuron response profiles (see Fig. 3), we performed a sliding window analysis, comparing responses in overlapping 500 ms bins to baseline using a paired samples t test. Figure 4A,B shows the number of neurons that responded significantly to odors A and B as a function of time following stimulus delivery. Overall, each odor evoked sparse responses in pPC (up to 20% of total neurons at any point in time during the stimulus period), in line with previous work using orthonasal as well as retronasal odorants. The number of neurons did not differ between odors, or between pre and post conditioning (χ^2 test: $p > 0.05$ for all time windows).
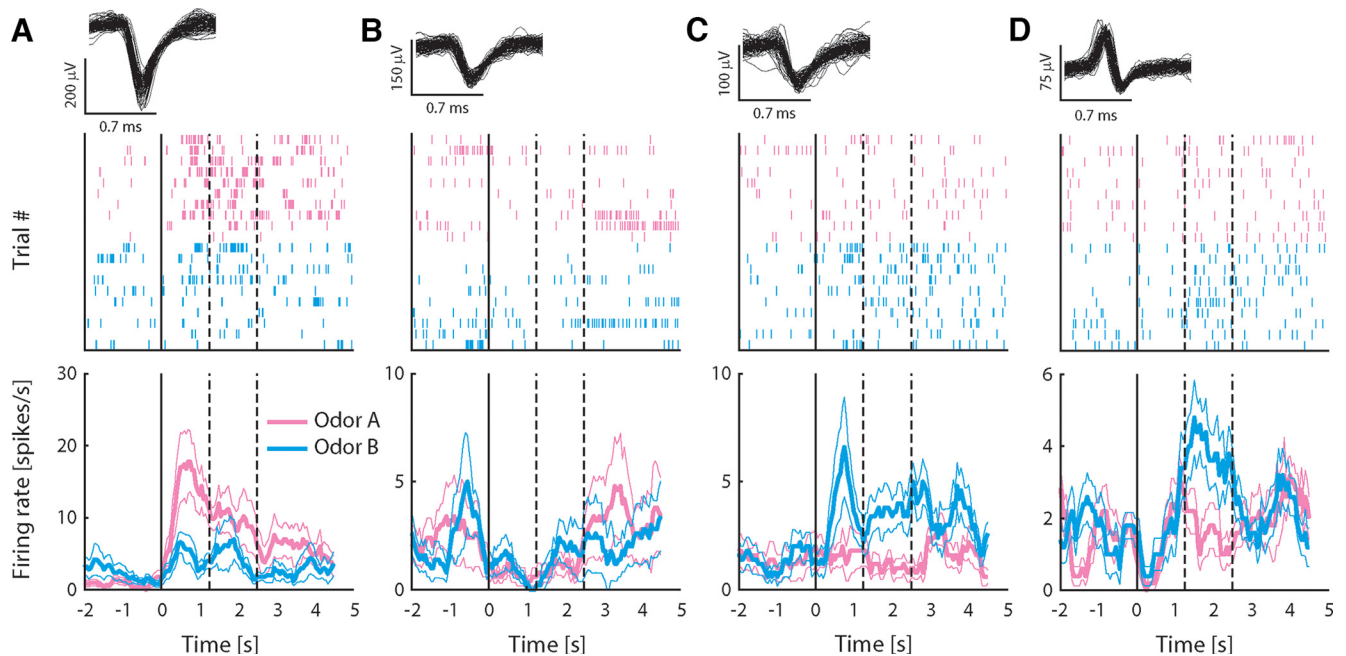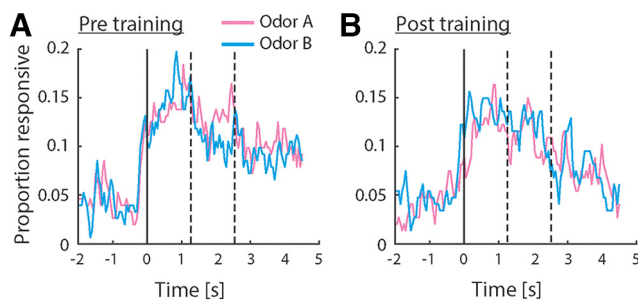
Figure 3. Responses to intraoral odor solutions recorded from exemplar pPC neurons. **A–D,** Top panels show 100 randomly selected waveforms (gray) in the single neuron cluster; middle panels are spike raster plots showing all action potentials for all trials aligned on stimulus delivery ($t = 0$); and bottom panels show average firing rate ($\pm$SEM) over trials in response to odors A and B. Rate plots are calculated using a 500-ms sliding window to illustrate the temporal profile of responses, but lack the temporal resolution of raster plots because of the size of the smoothing window. Neurons in **A, B** were recorded before conditioning; neurons in **C, D** after conditioning. Dashed lines indicate offset of "early" and "late" response epochs.
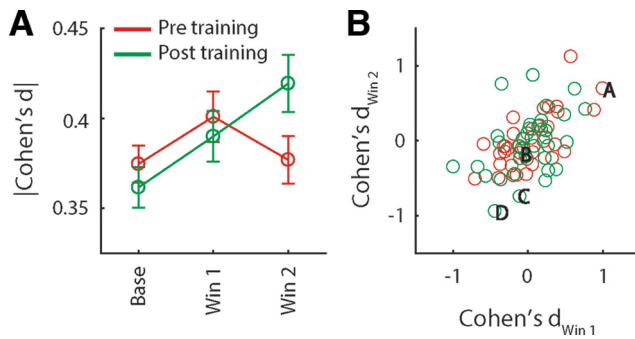
Dynamics of odor selectivity in single pPC neurons change after conditioning

The example responses shown in Figure 3 demonstrate that single pPC neuron responses can respond to multiple odors in a more or less selective manner. This pattern is generally in line with previous work using orthonasal odorants showing that different odors elicit responses in partly overlapping ensembles of piriform cortex neurons. To determine how well individual neurons distinguish between odors A and B, we analyzed neurons that exhibited significant overall responsiveness, defined as a significant

Figure 4. Odor responsiveness in the population of pPC neurons. **A, B,** Proportion of pPC neurons exhibiting a significant response relative to baseline, before (**A**) and after (**B**) conditioning. Responsiveness was calculated using a 500-ms sliding window. Dashed lines indicate offset of "early" and "late" response epochs. No significant differences in responsiveness were observed (χ^2 test comparing proportions between groups).

response to odor (pooled across odors A and B) in the stimulus period versus baseline ($n = 36$ neurons before and after conditioning). Cohen's d was used as a continuous measure of discriminability. We calculated discriminability in two time windows (0–1250 and 1250–2500 ms following stimulus delivery). Figure 5A shows average discriminability before and after conditioning during the early and late time windows, as well as during the baseline period. Two-way ANOVA on the magnitude of discriminability (i.e., the absolute value of Cohen's d) with factors Window (early, late) and Epoch (pre, post) revealed a significant Window $\times$ Epoch interaction ($F_{(1,279)} = 4.48$, $p < 0.05$). *Post hoc* comparisons (Bonferroni corrected) indicated that discriminability was significantly increased during the early portion of the response relative to baseline, and that during the late portion of the response, discriminability was significantly higher post versus pre conditioning. The increase in discriminability late in the response observed after conditioning could be the result of two scenarios. First, individual neurons could sustain their activity patterns established early in response (e.g., the neuron shown in Fig. 3C that prefers odor B over A during both the early and late portion of the response). Alternatively, activity patterns could differ between the early and late portion of the response (e.g., the neuron shown in Fig. 3D that is nonselectively early in the response, followed by an increase in firing rate in response to odor B over A later in the response). In the first scenario, raw Cohen's d values obtained from the two response windows would be highly correlated.
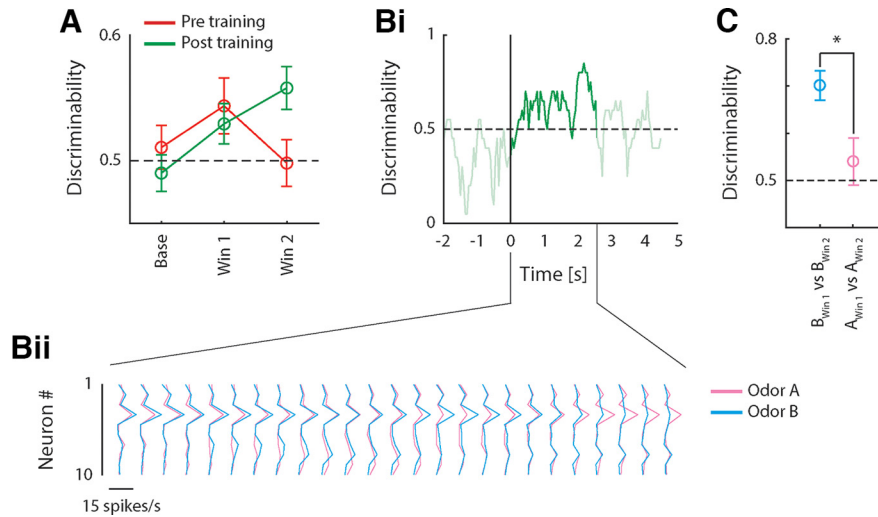
Figure 5. Discriminability between odors *A*, *B* at the single neuron level. *A*, Effect size (Cohen's *d*) of the difference in the response to odors A and B, averaged (±SEM) over all neurons recorded before and after conditioning ($n = 152$ and 147, respectively), during baseline, and early and late stimulus response epochs. *B*, Cohen's *d* obtained from the early and late response epochs for all odor-responsive neuron ($n = 36$ before and after conditioning). Letters correspond to the example responses in Figure 3.

That is, the early and late portions of the response should exhibit similar odor selectivity. In the second scenario, raw Cohen's *d* values obtained from the two response windows may be unrelated or even anticorrelated. Figure 5*B* shows raw Cohen's *d* values obtained from the two response windows for all stimulus responsive neurons recorded pre and post conditioning. Pre conditioning, odor discriminability is highly correlated between the two response windows ($r = 0.68$, $p < 0.001$), suggesting that odor selectivity established early in the response is to some extent sustained during the late portion of the response. Post conditioning, correlation between the two response windows is significantly reduced (*F* test comparing correlations obtained pre and post conditioning: $z = 1.78$, $p < 0.05$), despite the fact that discriminability is significant in the late portion of the response, and is, if anything, increased relative to the early portion of the response. This pattern of results is consistent with the second scenario, in which odor-evoked responses undergo pronounced qualitative changes over the course of the response post conditioning. Thus, odor-taste conditioning is associated with changes in the pattern of responses during the late epoch, such that odor discriminability is increased.

Odor information is present in single trial pPC ensemble responses

The analyses described above assessed responsiveness and discriminability of odors A and B at the level of single pPC neurons that were selected based on arbitrary response properties (i.e., significant responsiveness vs baseline). However, across the population of animals, few neurons exhibited significant responses, and the analysis presented above thus only takes into account a small sample of the total recorded neural activity. Next, we applied a more inclusive analysis, using all simultaneously recorded neural activity during individual sessions to determine whether odor identity could be decoded from the

complete ensemble response on a single-trial basis. This analysis takes into account subtle variations in responses across conditions, and trials within conditions, variability that is lost in the single-neuron-based analyses presented above, and thus more closely mimics real-world conditions where animals need to identify an odor during a single encounter using the entire population of pPC responses. For each odor, we calculated an ensemble response profile consisting of a vector of firing rates (one for each simultaneously-recorded neuron, averaged across the stimulus period). Discriminability of odors A and B was calculated by comparing the distance between each single-trial ensemble response profile and each of two trial-averaged ensemble response templates (one for odor A; one for odor B). A trial was classified correctly if the distance between the trial and the matching template was smallest (i.e., when the distance between an odor A trial and the odor A template was smaller than the distance between the odor A trial and the odor B template, and vice versa). Figure 6*A* shows the average decoding performance over all sessions that featured at least two simultaneously recorded neurons [$n = 20$ sessions both pre and post conditioning; mean number of neurons per ensemble (pre/post): 6.3/6.7; range: 2–16/2–12]. Overall, the pattern of results is consistent with the one obtained from single neurons (see Fig. 5*A*): early in the response, ensembles recorded both pre and post conditioning performed above chance. However, whereas decoding performance pre conditioning dropped during the late portion of the response, performance post conditioning remained high. This pattern was confirmed by ANOVA, revealing a Window × Epoch interaction ($F_{(1,37)} = 5.79$, $p < 0.05$). Next, we examined more closely the firing rate patterns on which decoding performance is based. Figure 6*Bi* shows decoding performance obtained from an example ensemble of 10 simultaneously recorded neurons post conditioning in a sliding window over time. The dynamics of the binned ensemble response during the stimulus period is shown in Figure 6*Bii*. Although decoding performance was mostly above chance during the entire stimulus period, response patterns underwent profound changes over the course of the response, such that neurons preferring odor A early in the response switch to preferring odor B later in the response, and vice versa. Such changes in selectivity are consistent with the results from the single neuron analysis presented above (see Fig. 5*B*), suggesting that odor representations change over the course of the response. To directly test whether this is true at the ensemble level, we compared single-trial ensemble responses to the same odor between two time windows (one early in the response; one late in the response). In other words, we asked the question: How well can we decode odor identity from late epoch ensemble responses using templates obtained from the early epoch? Figure 6*C* shows the result of this analysis. Ensemble responses to odor B during early and late epochs were easily distinguished, indicating that responses to odor B differed between epochs. In contrast, ensemble responses to odor A were more similar between epochs (*t* test comparing discriminability of

Figure 6. Single-trial decoding of odor identity from ensemble responses. ***A***, Discriminability between odors A and ***B***, averaged (±SEM) over all sessions with $n > 1$ neurons before and after conditioning ($n = 20$), during baseline, and early and late stimulus response epochs. ***Bi***, Discriminability as a function of time for an example ensemble recorded after conditioning ($n = 10$ neurons). Stimulus period (2500 ms following stimulus onset) is highlighted. ***Bii***, Firing rate patterns for all neurons in the example ensemble shown in ***Bi***. Responses are shown in a series of sliding windows (500-ms window size, 100-ms step size). ***C***, Discriminability of ensemble responses to the same odor in different response epochs. *t test: $p < 0.05$.

early and late epoch responses between odors A and B: $t_{(12)} = 2.46$, $p < 0.05$. No differences were found in between-epoch discriminability of responses to the same odors pre conditioning, a pattern that differed significantly from the one observed post conditioning (t test comparing the difference in discriminability between odors A and B pre versus post conditioning: $t_{(19)} = 2.60$, $p < 0.05$). Together, results from the decoding analysis demonstrate that odor identity can be read out early in the response using relatively small ensembles of pPC neurons, regardless of conditioning. Conditioning further enhances discriminability between conditioned and unconditioned odors in a manner that is selective to the late response epoch, and is characterized by a unique ensemble response code.

Ensemble decoding accuracy does not depend on palatability

The results presented above indicate that taste-odor association learning increases discriminability between the representations of odors A and B in the late portion of pPC ensemble responses. However, it is unclear what aspect of odors is reflected exactly in the response of pPC neurons. One possibility is that the late response epoch reflects odor palatability. Our behavioral results (Fig. 2) show that the palatability of the saccharin-associated odor increases after conditioning, and this increase in palatability could therefore be driving changes in pPC ensemble response patterns. To directly test for this possibility, we performed linear regression of ensemble discriminability during the late epoch on preference for odor B (Fig. 7A). This analysis yielded no significant effect of preference on odor discriminability ($F = 1.46$, $p = 0.24$). Regression using pre versus post conditioning as a predictor (Fig. 7B) confirmed that discriminability increased following association learning ($F = 5.70$,

$p < 0.05$). Thus, these findings suggest that ensemble discriminability cannot be explained by odor palatability, but instead reflects other aspects of odor perception.

Discussion

Our results demonstrate that taste-odor association learning changes responses of pPC neurons to odor solutions. Association-related changes in responsiveness appeared as changes in the dynamics of stimulus-evoked responses, leading to enhanced discriminability between representations of taste-associated and nontaste-associated odors. Learning-related activity patterns were selective to the late portion of the response, and qualitatively different from the patterns observed during the early portion of the response. We speculate that during oral evaluation of odor stimuli, association-related representations
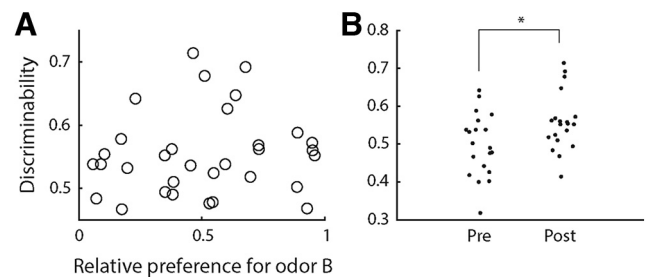
Figure 7. Relation between ensemble decoding accuracy and odor palatability. ***A***, Ensemble discriminability between odors A and B during the late response epoch as a function of relative preference for odor B for each animal ($n = 19$). No significant relation was detected by linear regression. ***B***, Ensemble discriminability between odors A and B during the late response epoch before and after conditioning for each animal ($n = 19$). *Regression: $p < 0.05$.

are generated by ongoing interactions with the taste system and can be read-out by downstream brain areas independently of chemical identity representations.

Experience-dependent coding of olfactory information is supported by the organization of the primary olfactory (piriform) cortex. Information about odorant identity is relayed from olfactory sensory neurons to the piriform cortex via the olfactory bulb, and is represented in unique but partly overlapping ensembles of neurons that are distributed throughout the piriform cortex without apparent spatial organization (Scott et al., 1980; Schwob and Price, 1984; Rennaker et al., 2007; Stettler and Axel, 2009; Miyamichi et al., 2011; Sosulski et al., 2011). Besides bottom-up sensory input from the olfactory bulb, piriform cortex also receives inputs from various extraolfactory systems (Luskin and Price, 1983; Johnson et al., 2000; Haberly, 2001; Majak et al., 2004; Sadrian and Wilson, 2015). Our findings are generally in line with previous work demonstrating that experience can shape cortical odor representations (Kadohisa and Wilson, 2006; W. Li et al., 2006, 2008; Calu et al., 2007; Roesch et al., 2007; Barnes et al., 2011; Chen et al., 2011; Chapuis and Wilson, 2012; Gire et al., 2013; Meissner-Bernard et al., 2019; D. Wang et al., 2019), and shed new light on the mechanisms underlying context-dependent cortical olfactory coding. One possible way of encoding experience is through plasticity in the local cortical circuit. In this scenario, experience affects how bottom-up inputs from the bulb are processed by the local cortical circuit, resulting in a static rearrangement of odor relationships. For example, Chapuis and colleagues (Chapuis and Wilson, 2012) showed that cortical representations of the components of an odor mixture may become more or less similar to each other, depending on whether rats were rewarded to respond to the mixture in a configural or elemental manner, respectively. In addition to experience-dependent changes in the local representation of bottom-up input patterns, some studies have suggested that piriform cortex may explicitly encode associative features of odor stimuli independently of chemical identity (Calu et al., 2007; Roesch et al., 2007; Gire et al., 2013; Meissner-Bernard et al., 2019; D. Wang et al., 2019). Conversely, others have suggested that explicit encoding of associative features occurs elsewhere in the brain (Millman and Murthy, 2020; P.Y. Wang et al., 2020).

The present findings suggest that pPC neurons explicitly encode taste associations of odors in the temporal dynamics of their response, uncovering new insight into the mechanisms underlying context-dependent cortical odor coding. Experience-dependent changes did not appear as static changes in odor representations. That is, changes were not uniform across the response period. Instead, experience-dependent changes were confined to the late portion of the response. Changes in response dynamics following conditioning did not simply sustain the representation observed during the early portion of the response, but led to the emergence of a new representation. Taken together, these findings suggests that pPC neurons multiplex information using a dynamic coding scheme, where different

aspects of an odor stimulus are represented during different epochs over the course of the response. With respect to the early response period (initial 1 s following stimulus delivery), we speculate, in line with previous work on piriform cortical odor coding, that activity patterns reflect bottom-up input from the olfactory bulb containing information about odor identity (Rennaker et al., 2007; Poo and Isaacson, 2009; Stettler and Axel, 2009; Bolding and Franks, 2017). With respect odor information that appeared selectively after conditioning during the late response period (after 1 s following stimulus deliver), activity patterns may encode taste associations of odors; alternatively, they may reflect hedonic value of odors. The former interpretation is consistent with the proposed role for piriform cortex in stimulus identity processing, and pPC neurons may dynamically represent chemical odor identity and associated taste identity. Indeed, behavioral work in humans suggests that taste associations of odors can be taste specific (Stevenson et al., 1995, 1998, 2000a, b; Stevenson and Boakes, 2004; Yeomans et al., 2006). Moreover, we did not find any evidence that the late portion of the pPC response reflects odor palatability. Future work in which animals learn to associate different odors with different tastes that vary in quality and hedonic value will more explicitly characterize the nature of information encoded in the different response epochs.

Few studies to date have explicitly considered the temporal dynamics of cortical odor responses and their relation to associative coding. One notable exception is a study by Gire and colleagues (Gire et al., 2013), who recorded from neurons in the posterior piriform cortex of rats to rewarded and unrewarded odors. They considered the contribution of activity patterns at two temporal scales: inhalation-locked and noninhalation-locked. Whereas information about chemical identity was present in fast, inhalation-locked responses that are thought to reflect processing of bottom-up inputs by local piriform cortical circuits (Bolding and Franks, 2018), information about reward value was present in slower activity patterns that were not locked to respiration. The slow dynamics of experience-dependent activity pattern observed in the present study and by Gire et al. (2013) suggests that they are conveyed to pPC by top-down inputs. Together, findings from both studies support a model in which associative odor coding emerges dynamically through ongoing interactions with extraolfactory systems. More broadly, a dynamic model of odor coding in pPC is in line with previous observations of response dynamics at time scales beyond the sniff cycle (Rennaker et al., 2007; D. Wang et al., 2019).

Dynamic multiplexing of sensory and associative information at timescales similar to the ones observed in the present study has previously been observed in other brain regions that process consumption-related sensory cues. For example, activity patterns in the insular gustatory cortex reflect taste identity during the initial second following intraoral taste delivery; followed by activity patterns that reflect hedonic value of the taste stimulus, independent of stimulus identity (Katz et al., 2001; Sadacca et al., 2012).

Moreover, EMG recordings of orofacial movements in response to intraoral taste solutions demonstrate that changes in GC neuron response patterns precede the expression of palatability-related behavioral responses, suggesting a causal role for response dynamics in controlling behavior (J.X. Li et al., 2016; Mukherjee et al., 2019). These response dynamics arise from ongoing interactions with the basolateral amygdala (Fontanini et al., 2009; Piette et al., 2012; Lin et al., 2021). In the present study, we did not measure behavioral responses on a trial-by-trial basis, but the temporal scale of the observed dynamics is broadly consistent with a role in oral evaluation of sensory stimuli. Future work measuring orofacial movements (e.g., mouth movements, sniffing) in real time will determine the temporal relation between behavioral and neural response patterns.

The effects of conditioning observed in the present study constitute relatively subtle changes in neural response patterns. Odor responsiveness in individual neurons was overall sparse, and conditioning did not result in significant changes in responsiveness of individual neurons (i.e., we did not observe an increase or decrease in the number of neurons that responded significantly to odor stimuli). The lack of sensitivity in single neuron analysis may be because of a high degree of response variability. One factor that likely contributed to response variability across trials is the protracted nature of the response. Responses of single pPC neurons unfolded over seconds following stimulus delivery and are poorly locked to stimulus onset. Another source of variability is that neural activity appeared to change in a heterogenous manner, with some neurons increasing and others decreasing their activity levels in a dynamic manner. These issues underscore the value of ensemble analysis that takes into account correlated, heterogeneous changes in neural activity across multiple neurons on a single trial basis. Indeed, our ensemble decoding analysis was able to significantly discriminate between odor representations using responses from relatively small ensembles of pPC neurons.

The changes in pPC responsiveness following taste association learning observed here are reminiscent of the changes in pPC responses to odor solutions when presented in mixture with taste compounds. We recently demonstrated that taste and odor components of mixtures interact to change responses of pPC neurons in real time (Idris et al., 2023). Multisensory modulations observed in that study resembled the experience-dependent modulations observed here in that they were mostly subtle at the single neuron level, heterogenous in nature, and led to greater discriminability of odor representations at the ensemble level. Also in line with the present findings, increased discriminability resulting from real-time multisensory modulation was not observed until later in the response, following an initial unisensory odor-selective phase. The fact that we recorded from separate populations of neurons before and after conditioning precludes a direct comparisons between real-time and experience-driven pPC response modulation, future work aimed at tracking the activity of single neurons across conditioning will determine whether real-time interactions between taste and smell components of mixture are predictive of experience-dependent modulations.

Regarding potential extraolfactory sources relaying associative input about taste, previous work has identified GC as a candidate region, as inactivation of GC prohibited the expression of preferences for sweet taste-associated odors (Maier et al., 2015; Blankenship et al., 2019). Based on previous findings, the influence of GC on olfactory processing appears to be specific to the context of consumption. Intraoral delivery of odors in solution creates a unique context that has been shown to play a key role in mediating taste-odor association learning. Blankenship et al. (2019) demonstrated that animals more readily learn preferences for sweet taste-associated odor when odors were presented intraorally versus orthonasally, and that inactivating GC selectively affected the expression of preferences for intraorally presented sweet taste-associated odors. Further evidence for unique processing of consumption-related odor signals comes from human imaging work, showing increased BOLD signal in GC in response to food odors versus non-food odors (Veldhuizen et al., 2010). Although it remains unclear whether the response patterns observed in the present study are unique to the context of consumption, pPC neurons have been shown to be sensitive to oral context: responses to the same odorant presented intraorally and orthonasally can differ substantially (Maier, 2017). Together, these findings suggest that oral context may play a key role in generating the response patterns observed in the present study.

References

Avery JA, Liu AG, Ingeholm JE, Riddell CD, Gotts SJ, Martin A (2020) Taste quality representation in the human brain. J Neurosci 40:1042–1052.

Barnes DC, Chapuis J, Chaudhury D, Wilson DA (2011) Odor fear conditioning modifies piriform cortex local field potentials both during conditioning and during post-conditioning sleep. PLoS One 6:e18130.

Blankenship ML, Grigorova M, Katz DB, Maier JX (2019) Retronasal odor perception requires taste cortex, but orthonasal does not. Curr Biol 29:62–69.e3.

Bolding KA, Franks KM (2017) Complementary codes for odor identity and intensity in olfactory cortex. Elife 6:e22630.

Bolding KA, Franks KM (2018) Recurrent cortical circuits implement concentration-invariant odor coding. Science 361:eaat6904.

Bushdid C, Magnasco MO, Vosshall LB, Keller A (2014) Humans can discriminate more than 1 trillion olfactory stimuli. Science 343:1370–1372.

Calu DJ, Roesch MR, Stalnaker TA, Schoenbaum G (2007) Associative encoding in posterior piriform cortex during odor discrimination and reversal learning. Cereb Cortex 17:1342–1349.

Chapuis J, Wilson DA (2012) Bidirectional plasticity of cortical pattern recognition and behavioral sensory acuity. Nat Neurosci 15:155–161.

Chen CF, Barnes DC, Wilson DA (2011) Generalized vs. stimulus-specific learned fear differentially modifies stimulus encoding in primary sensory cortex of awake rats. J Neurophysiol 106:3136–3144.

Christensen BA, Triplett CS, Maier JX (2022) Odor mixture perception during flavor consumption in rats. Behav Neurosci 136:300–306.

Elliott VE, Maier JX (2020) Multisensory interactions underlying flavor consumption in rats: the role of experience and unisensory component liking. Chem Senses 45:27–35.

Fontanini A, Grossman SE, Figueroa JA, Katz DB (2009) Distinct sub-types of basolateral amygdala taste neurons reflect palatability and reward. J Neurosci 29:2486–2495.

Gadziola MA, Tylicki KA, Christian DL, Wesson DW (2015) The olfactory tubercle encodes odor valence in behaving mice. J Neurosci 35:4515–4527.

Gautam SH, Verhagen JV (2012) Direct behavioral evidence for retro-nasal olfaction in rats. PLoS One 7:e44781.

Gire DH, Whitesell JD, Doucette W, Restrepo D (2013) Information for decision-making and stimulus identification is multiplexed in sensory cortex. Nat Neurosci 16:991–993.

Haberly LB (2001) Parallel-distributed processing in olfactory cortex: new insights from morphological and physiological analysis of neuronal circuitry. Chem Senses 26:551–576.

Holman E (1975) Immediate and delayed reinforcers for flavor prefer-ences in rats. Learn Motiv 6:91–100.

Idris A, Christensen BA, Walker EM, Maier JX (2023) Multisensory in-tegration of orally-sourced gustatory and olfactory inputs to the posterior piriform cortex in awake rats. J Physiol 601:151–169.

Johnson DM, Illig KR, Behan M, Haberly LB (2000) New features of connectivity in piriform cortex visualized by intracellular injection of pyramidal cells suggest that "primary" olfactory cortex functions like "association" cortex in other sensory systems. J Neurosci 20:6974–6982.

Kadohisa M, Wilson DA (2006) Separate encoding of identity and similarity of complex familiar odors in piriform cortex. Proc Natl Acad Sci U S A 103:15206–15211.

Karunanayaka PR, Wilson DA, Vasavada M, Wang J, Martinez B, Tobia MJ, Kong L, Eslinger P, Yang QX (2015) Rapidly acquired multisensory association in the olfactory cortex. Brain Behav 5: e00390.

Katz DB, Simon SA, Nicolelis MA (2001) Dynamic and multimodal re-sponses of gustatory cortical neurons in awake rats. J Neurosci 21:4478–4489.

Li JX, Maier JX, Reid EE, Katz DB (2016) Sensory cortical activity is related to the selection of a rhythmic motor action pattern. J Neurosci 36:5596–5607.

Li W, Luxenberg E, Parrish T, Gottfried JA (2006) Learning to smell the roses: experience-dependent neural plasticity in human piri-form and orbitofrontal cortices. Neuron 52:1097–1108.

Li W, Howard JD, Parrish TB, Gottfried JA (2008) Aversive learning enhances perceptual and cortical discrimination of indiscriminable odor cues. Science 319:1842–1845.

Lin JY, Mukherjee N, Bernstein MJ, Katz DB (2021) Perturbation of amygdala-cortical projections reduces ensemble coherence of palatability coding in gustatory cortex. Elife 10:e65766.

Luskin MB, Price JL (1983) The topographic organization of associa-tional fibers of the olfactory system in the rat, including centrifugal fibers to the olfactory bulb. J Comp Neurol 216:264–291.

Maier JX (2017) Single-neuron responses to intraoral delivery of odor solutions in primary olfactory and gustatory cortex. J Neurophysiol 117:1293–1304.

Maier JX, Elliott VE (2020) Adaptive weighting of taste and odor cues during flavor choice. J Neurophysiol 124:1942–1947.

Maier JX, Blankenship ML, Li JX, Katz DB (2015) A multisensory net-work for olfactory processing. Curr Biol 25:2642–2650.

Majak K, Rönkkö S, Kemppainen S, Pitkänen A (2004) Projections from the amygdaloid complex to the piriform cortex: a PHA-L study in the rat. J Comp Neurol 476:414–428.

McQueen KA, Fredericksen KE, Samuelsen CL (2020) Experience in-forms consummatory choices for congruent and incongruent odor-taste mixtures in rats. Chem Senses 45:371–382.

Meissner-Bernard C, Dembitskaya Y, Venance L, Fleischmann A (2019) Encoding of odor fear memories in the mouse olfactory cor-tex. Curr Biol 29:367–380.e4.

Millman DJ, Murthy VN (2020) Rapid learning of odor-value associa-tion in the olfactory striatum. J Neurosci 40:4335–4347.

Miyamichi K, Amat F, Moussavi F, Wang C, Wickersham I, Wall NR, Taniguchi H, Tasic B, Huang ZJ, He Z, Callaway EM, Horowitz MA,

Luo L (2011) Cortical representations of olfactory input by trans-synaptic tracing. Nature 472:191–196.

Mukherjee N, Wachutka J, Katz DB (2019) Impact of precisely-timed inhibition of gustatory cortex on taste behavior depends on single-trial ensemble dynamics. Elife 8:e45968.

Paxinos G, Watson C (1986) The rat brain atlas. San Diego: Academic Press, Inc.

Phillips MI, Norgren RE (1970) A rapid method for permanent implan-tation of an intraoral fistula in rats. Behav Res Methods 2:124.

Piette CE, Baez-Santiago MA, Reid EE, Katz DB, Moran A (2012) Inactivation of basolateral amygdala specifically eliminates palata-bility-related information in cortical sensory responses. J Neurosci 32:9981–9991.

Poo C, Isaacson JS (2009) Odor representations in olfactory cortex: "sparse" coding, global inhibition, and oscillations. Neuron 62:850–861.

Quiroga RQ, Reddy L, Koch C, Fried I (2007) Decoding visual inputs from multiple neurons in the human temporal lobe. J Neurophysiol 98:1997–2007.

Rennaker RL, Chen CF, Ruyle AM, Sloan AM, Wilson DA (2007) Spatial and temporal distribution of odorant-evoked activity in the piriform cortex. J Neurosci 27:1534–1542.

Roesch MR, Stalnaker TA, Schoenbaum G (2007) Associative en-coding in anterior piriform cortex versus orbitofrontal cortex during odor discrimination and reversal learning. Cereb Cortex 17:643–652.

Rossant C, Kadir SN, Goodman DFM, Schulman J, Hunter MLD, Saleem AB, Grosmark A, Belluscio M, Denfield GH, Ecker AS, Tolias AS, Solomon S, Buzsaki G, Carandini M, Harris KD (2016) Spike sorting for large, dense electrode arrays. Nat Neurosci 19:634–641.

Sadacca BF, Rothwax JT, Katz DB (2012) Sodium concentration coding gives way to evaluative coding in cortex and amygdala. J Neurosci 32:9999–10011.

Sadrian B, Wilson DA (2015) Optogenetic stimulation of lateral amyg-dala input to posterior piriform cortex modulates single-unit and ensemble odor processing. Front Neural Circuits 9:81.

Schwob JE, Price JL (1984) The development of axonal connections in the central olfactory system of rats. J Comp Neurol 223:177–202.

Sclafani A, Ackroff K (1994) Glucose- and fructose-conditioned fla-vor preferences in rats: taste versus postingestive conditioning. Physiol Behav 56:399–405.

Scott JW, McBride RL, Schneider SP (1980) The organization of pro-jections from the olfactory bulb to the piriform cortex and olfactory tubercle in the rat. J Comp Neurol 194:519–534.

Slotnick BM, Westbrook F, Darling FMC (1997) What the rat's nose tells the rat's mouth: long delay aversion conditioning with aque-ous odors and potentiation of taste by odors. Anim Learn Behav 25:357–369.

Sosulski DL, Bloom ML, Cutforth T, Axel R, Datta SR (2011) Distinct representations of olfactory information in different cortical centres. Nature 472:213–216.

Stettler DD, Axel R (2009) Representations of odor in the piriform cor-tex. Neuron 63:854–864.

Stevenson R, Boakes R (2004) Sweet and sour smells: learned syn-aesthesia between the senses of taste and smell. In: The hand-book of multisensory processing (Calvert G, Spence C, Stein B, eds), pp 69–83. Cambridge: MIT Press.

Stevenson R, Prescott J, Boakes R (1995) The acquisition of taste properties by odors. Learn Motiv 26:433–455.

Stevenson RJ, Boakes RA, Prescott J (1998) Changes in odor sweet-ness resulting from implicit learning of a simultaneous odor-sweet-ness association: an example of learned synesthesia. Learn Motiv 29:113–132.

Stevenson RJ, Boakes RA, Wilson JP (2000a) Counter-conditioning following human odor–taste and color–taste learning. Learn Motiv 31:114–127.

Stevenson RJ, Boakes RA, Wilson JP (2000b) Resistance to ex-tinction of conditioned odor perceptions: evaluative

conditioning is not unique. J Exp Psychol Learn Mem Cogn 26:423–440.

Veldhuizen MG, Nachtigal D, Teulings L, Gitelman DR, Small DM (2010) The insular taste cortex contributes to odor quality coding. Front Hum Neurosci 4:58.

Wang D, Liu P, Mao X, Zhou Z, Cao T, Xu J, Sun C, Li A (2019) Task-demand-dependent neural representation of odor information in the olfactory bulb and posterior piriform cortex. J Neurosci 39:10002–10018.

Wang PY, Boboila C, Chin M, Higashi-Howard A, Shamash P, Wu Z, Stein NP, Abbott LF, Axel R (2020) Transient and persistent representations of odor value in prefrontal cortex. Neuron 108:209–224.e6.

Wilson DA, Stevenson RJ (2003) The fundamental role of memory in olfactory perception. Trends Neurosci 26:243–247.

Wilson DA, Best AR, Sullivan RM (2004) Plasticity in the olfactory system: lessons for the neurobiology of memory. Neuroscientist 10:513–524.

Yeomans MR, Mobini S, Elliman TD, Walker HC, Stevenson RJ (2006) Hedonic and sensory characteristics of odors conditioned by pairing with tastants in humans. J Exp Psychol Anim Behav Process 32:215–228.

Zelano C, Bensafi M, Porter J, Mainland J, Johnson B, Bremner E, Telles C, Khan R, Sobel N (2005) Attentional modulation in human primary olfactory cortex. Nat Neurosci 8:114–120.